

Robert M. Rauber, Mohan K. Ramamurthy, Brian F. Jewett, and Mei Han
 Department of Atmospheric Sciences
 University of Illinois at Urbana-Champaign, Urbana, IL

1. INTRODUCTION

It is well documented that the location of heavy snowfall in the northwest quadrant of continental winter cyclones is coincident with the position of an airstream aloft originating in the warm sector of the cyclone (e.g. Schultz and Mass 1993, Martin 1999). This airstream, termed the trough of warm air aloft, or trowal, has been shown in modeling studies to ascend within a wedge formed between the warm frontal surface to the north, and the advancing cold front aloft to the south (Martin 1998) in a manner reminiscent of early models of warm occluded structure. Isentropic trajectory analyses have shown that several airmasses, with different thermal and moisture characteristics, converge in this region (e.g. Martin 1999). When viewed with radar, the wide band of precipitation within the trowal is often composed of more intense, narrower bands. For example, in snowstorms discussed by Sanders and Bosart (1985) and Moore and Blakely (1988), “pulselike” oscillations in cloud top and banded structures were observed across the region of heavy snowfall. The mechanism most commonly invoked to explain these precipitation structures is the release of CSI (see Shultz and Schumacher 1999). Other mechanisms that may lead to multiple bands include gravity waves, melting induced circulations, and the release of convective instability in the boundary layer. The Snowband Dynamics Project (SNOWBAND) was designed to obtain a high resolution data set to investigate the fine scale structure and dynamics of the heavy snowbands within the northwest quadrant of cyclones. The project was carried out in cooperation with the Lake-Induced Convection Experiment (Kristovich et al. 2000) in the vicinity of Lake Michigan during the 1997-8 winter season. In this paper, the mesoscale structure and dynamical forcing of a heavy snowband that occurred over Michigan in the northwest quadrant of an extratropical cyclone is discussed. Cross-band wind and thermodynamic analyses derived from high resolution dropsonde data and WSR-88D analyses are combined with analyses from high-resolution MM5 modeling experiments to examine the key mechanisms forcing vertical motion within the snowstorm.

2. DATA ANALYSES

On 10 Dec 1997, a cyclone that had formed in the lee of the Rocky Mountains propagated northeastward through the Ohio valley. A band of heavy precipitation formed in its northwest quadrant, with some regions experiencing snowfall rates of 2-5 cm per hour for several hours, with over 30 cm falling in south-central Michigan. Fig. 1 shows the band at the time that the NCAR Electra dropped high resolution dropsondes along the path shown in Fig. 3. As shown on this figure, strong easterly surface winds were present north of a diffuse low pressure center located across Indiana and Ohio. Cross sections constructed from the dropsondes are shown on Fig. 2. A double frontal structure is evident in both the θ and θ_e fields, the uppermost front a warm front and the lower front associated with a secondary southward surge of colder air. The trowal appears above the uppermost frontal zone, bounded by the warm front to the north and the advancing dry slot to the south. The dry slot appears most prominently in the relative humidity field on the south (right) side of the cross section.

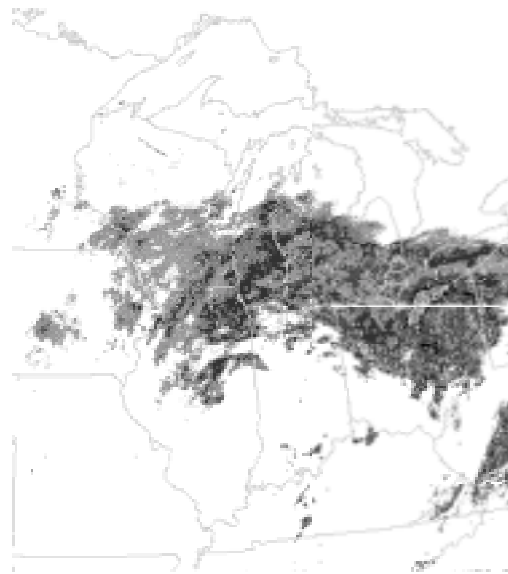


Fig. 1: Radar composite view of snowband over northern U.S. on 10 Dec 97 at 1400 UTC.

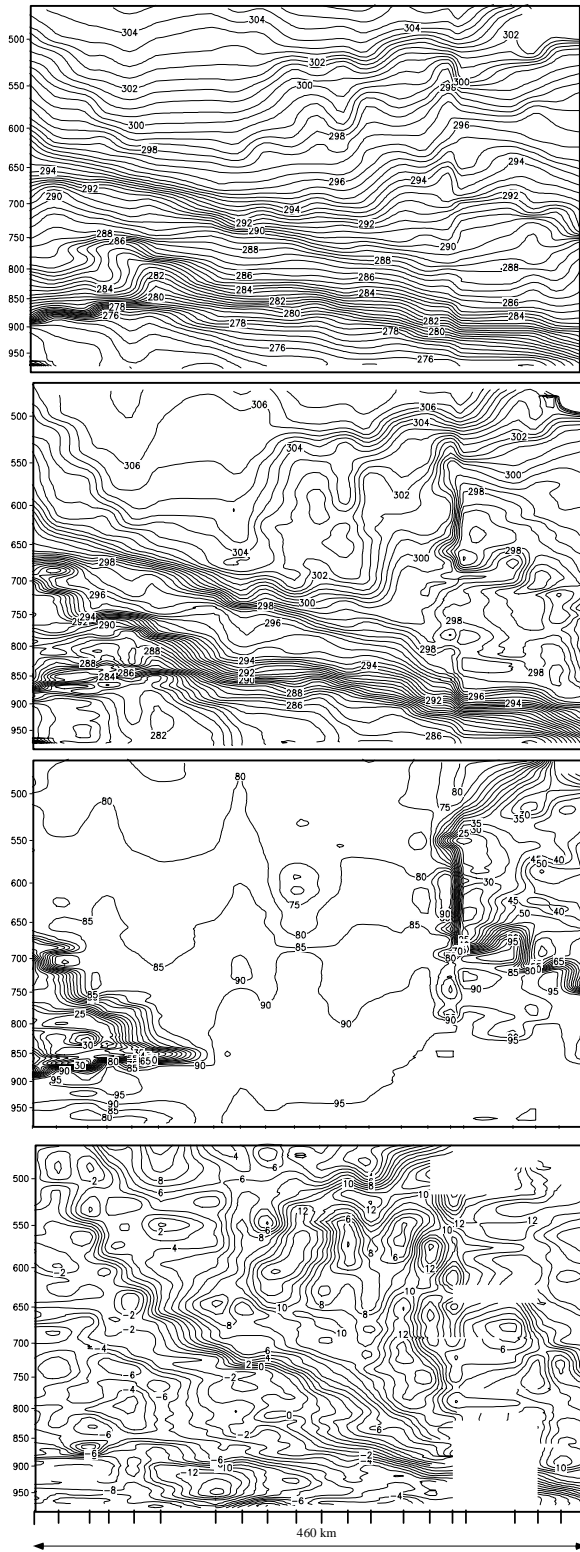


Fig. 2: Cross section of θ (K), θ_e (K), Relative Humidity (%) and tangential wind (m/s) along the line indicated in Fig. 3. The vertical lines denote the locations of the dropsondes.

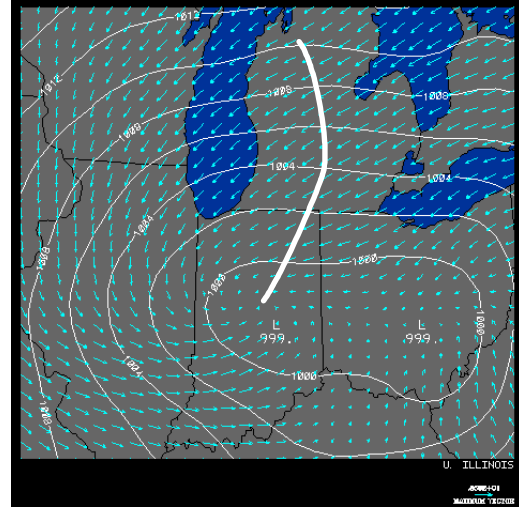


Fig. 3: Surface winds and pressure at 1400 UTC 10 Dec 1997. The line denotes the flight track during the dropsonde launch (see the cross section in Fig. 2).

Fine-scale wind variations, indicative of gravity waves, were north of the upper-level dry slot as well as along the frontal boundary to the north. These gravity waves are also evident in the θ field. Animations of the radar reflectivity factor from WSR-88Ds located along the band show reflectivity enhancements propagating in a wavelike manner from south to north across the band as the overall band underwent deformation. Analysis of the larger scale synoptic data (not shown), combined with the finescale data obtained from radar and dropsondes, suggest that the band developed as a result of ageostrophic circulations associated with frontogenesis and was modulated by gravity waves originating near the leading edge of the dry slot boundary and propagating northward across the trowal. This hypothesis is being tested in a series of MM5 simulations.

3. MM5 SIMULATIONS

The NCAR/Penn State MM5 Version 3 model has been used to simulate and understand the dynamical forcing of the heavy snowband occurring on 10 December 1997. Three nested domains, with 81, 27 and 9 km horizontal grid spacing and 46 vertical layers were employed. The innermost domain covered a 1600x1350 km region centered on Indiana. NCEP Global Data Assimilation System analyses were used for initial and boundary conditions on the outermost domain, while NCEP Rapid Update Cycle fields provided initial condition data on the inner two nested grids. The physics employed included simple ice (Dudhia) microphysics, Grell cumulus parameterization, Blackadar boundary layer and multi-layer soil model. Simulations were made for 24 hours starting at 0000 UTC 10 Dec.

Dataset: exp11d2 RIP: rip exp11d2 Init: 0000 UTC Wed 10 Dec 97
 Fcst: 16.00 Valid: 1600 UTC Wed 10 Dec 97 (1000 CST Wed 10 Dec 97)
 Sea-level pressure
 Surface air temperature

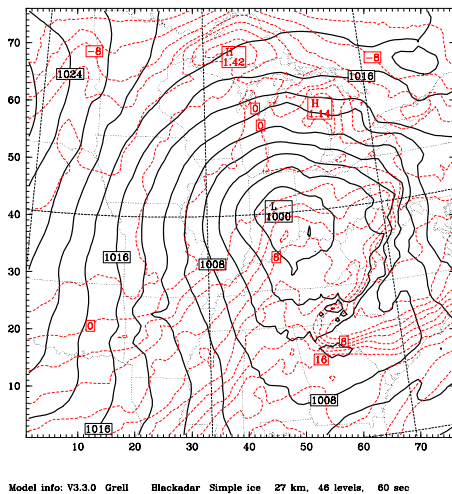


Figure 4: MM5 sea level pressure and surface air temperature at 1600 UTC 10 December 1997.

Dataset: exp11d2 RIP: rip exp11d2 Init: 0000 UTC Wed 10 Dec 97
 Fcst: 16.00 Valid: 1600 UTC Wed 10 Dec 97 (1000 CST Wed 10 Dec 97)
 Sea-level pressure
 Horizontal wind vectors at sigma = 0.996

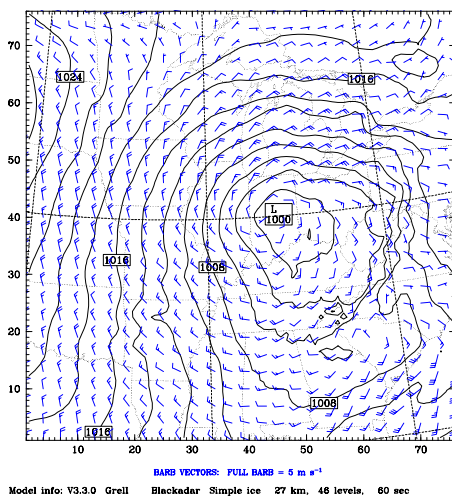


Figure 5: MM5 sea level pressure and wind at 1600 UTC 10 December 1997.

Analyses shown here were at 1600 UTC 10 Dec. As noted before, the observations suggest that the snowband developed as a result of ageostrophic circulations associated with frontogenesis but was modulated by smaller scale gravity waves. The scales inherent in these two types of motions are quite different. Our approach has been to analyze both quasi-geostrophic and ageostrophic frontogenetic circulations on the 27 km grid and gravity wave circulations on the 9 km grid. The Grid 2 results are summarized here. Grid 3 results will be presented at the conference. The results from Grid 2 were obtained using data that were filtered using a

cowbell filter, which suppresses features with scales smaller than 108 km ($4\Delta x$).

4. GENERAL FEATURES OF MM5 SIMULATION

Figures 4 and 5 show sea level pressure, surface temperature and wind from Grid 2. Figure 6 shows the rainwater and θ at 900 mb. Comparing Figs. 3 and 4, the model surface cyclone structure closely matched the intensity and location of the observed surface low pressure center. The model surface warm front developed at approximately the same location as the observed front, and its vertical thermodynamic and kinematic structure were reproduced reasonably well in model cross sections (compare the θ_e field in Fig. 8 with panel 2 of Fig. 2). Figure 6, the rainwater mixing ratio at 1600 UTC, shows the simulated band in a location approximately aligned with the observed band (see Fig. 1). Comparison of these analyses and other analyses of the upper atmospheric structure not shown (e.g. jetstream position, intensity and structure) suggest that the model simulation of the general features of the cyclone structure was sufficiently robust that meaningful analyses of the dynamic forcing of the band could be carried out.

5. DYNAMIC FORCING OF BAND-SCALE CIRCULATIONS

Fig. 7 shows the vertical motion (w_{dif}) associated with ageostrophic circulations in the region of the trowal. The vertical motion field was derived by subtracting the diagnosed quasi-geostrophic vertical motion from the total vertical motion calculated by the model. The axis of main w_{dif} extended along the trowal from near the warm frontal surface upward to approximately 400 mb.

Dataset: exp11d2 RIP: rip exp11d2 Init: 0000 UTC Wed 10 Dec 97
 Fcst: 16.00 Valid: 1600 UTC Wed 10 Dec 97 (1000 CST Wed 10 Dec 97)
 Rain water mixing ratio at pressure = 900 hPa
 Potential temperature at pressure = 900 hPa

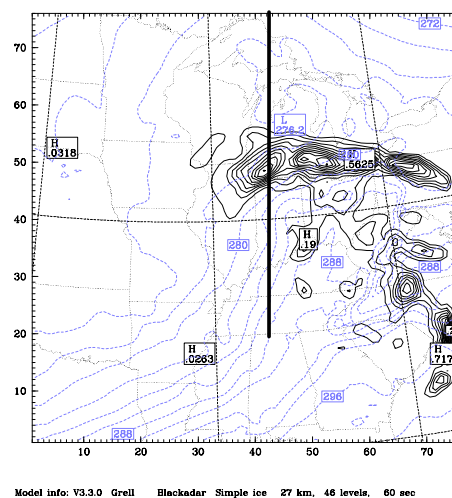


Figure 6: Rainwater mixing ratio and potential temperature (dashed) at 900 mb at 1600 UTC 10 December 1997.

Dataset: exp11d2 RIP: rip exp11d2 Init: 0000 UTC Wed 10 Dec 97
 Fcst: 16.00 Valid: 1600 UTC Wed 10 Dec 97 (1000 CST Wed 10 Dec 97)
 QC omega (dry) (Added field, factor of -1.00)
 Full-QG omega at pressure=700hpa qgsm=504

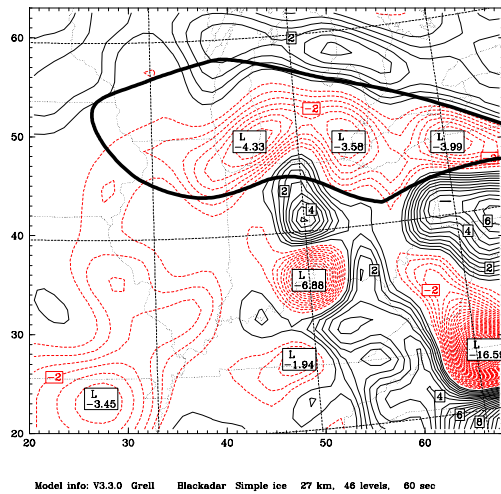


Figure 7: 700 mb vertical motion field obtained by subtracting the component of the vertical motion associated with quasi-geostrophic forcing from the total vertical motion predicted by the model. The dark line outlines the radar echoes appearing on Fig. 1.

Dataset: exp11d2 RIP: rip exp11d2 Init: 0000 UTC Wed 10 Dec 97
 Fcst: 16.00 Valid: 1600 UTC Wed 10 Dec 97 (1000 CST Wed 10 Dec 97)
 sep11111(al fnt=2) XY= 42.0, 75.0 to 42.0, 20.0 sm= 4
 Rain water mixing ratio XY= 42.0, 75.0 to 42.0, 20.0
 Equivalent potential temperature XY= 42.0, 75.0 to 42.0, 20.0

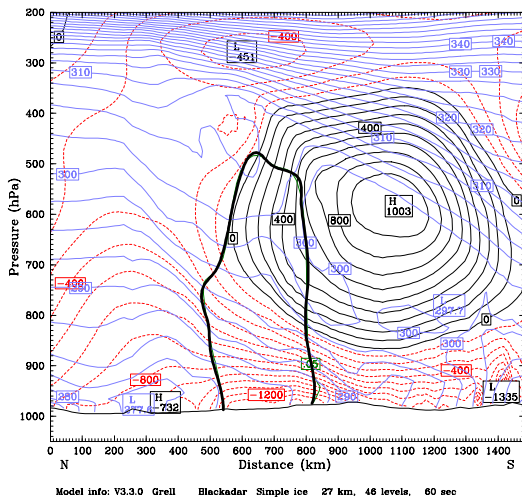


Figure 8: Vertical streamfunction obtained from solving the Sawyer-Eliassen equation in a plane oriented N-S across the precipitation band. The position of the band, indicated by the 0.01 g/kg rainwater contour, is near the center of the cross section. θ_e contours are also shown. The location of the cross section is shown on Fig. 6.

The forcing for this vertical motion was diagnosed by applying the geostrophic momentum approximation and solving the Sawyer-Eliassen equation for the 2-D streamfunction (ψ) in a N-S plane crossing the band (see Fig. 6). The lateral boundary conditions for ψ were determined by assuming the winds along the boundary

were geostrophic and computing $\partial\psi/\partial z$. The lower boundary condition considered terrain and friction, while the upper boundary condition was $\psi = 0$. Fig. 8 shows the derived streamfunction. Diabatic effects are not included in this figure. Also shown on Fig. 8 is the outer contour of the rainwater field. The simulated precipitation band formed within the southern side of the trowal as observed. The S-E circulation due to geostrophic shearing deformation within the trowal was frontogenetic. However, because of the orientation of the isotherms within the trowal and the presence of a strong jetstream to the south, a thermally direct circulation resulted in rising motion to the north and sinking to the south. On the other hand, the thermally direct circulation associated with geostrophic stretching deformation (which was also frontogenetical), produced rising motion to the south and descent to the north. The effects of shearing deformation were dominant, leading to the circulation in Fig. 8. Inclusion of condensation effects (not shown) enhanced the vertical motion along the band, but not significantly. More aspects of these simulations will be presented at the conference.

6. DYNAMIC FORCING OF SUB-BAND SCALE CIRCULATIONS

Preliminary analyses of sub-band circulations on the fine resolution grid suggest that gravity waves were generated in the trowal. The source, structure, and evolution of these waves and their relationship to precipitation are currently being studied. We believe that the gravity waves are being generated near the dry slot boundary due to strong wind shear across the boundary. In the radar reflectivity animations, waves appear to emanate from this boundary. This behavior is consistent with the waves appearing in the dropsonde cross section of both θ and the tangential wind component in Fig. 2A and 2D. Further information on this aspect of the study will be presented at the conference.

ACKNOWLEDGEMENTS

This work was funded by the NSF under grants NSF ATM 9708170 and NSF 0004274

REFERENCES

- Kristovich et al. 2000. *BAMS.*, **81**, 519-542.
- Martin, J. E., 1998: *Mon. Wea. Rev.*, **126**, 303-328.
- Martin, J. E., 1999a: *Mon. Wea. Rev.*, **127**, 70-88.
- Moore, J. T., and P. D. Blakely, 1988: *Mon. Wea. Rev.*, **116**, 2155-2171.
- Sanders, F., and L. F. Bosart, 1985: *J. Atmos. Sci.*, **42**, 1050-1061.
- Schultz, D.M., and C.F. Mass, 1993: *Mon. Wea. Rev.*, **121**, 918-940.
- Schultz, D.M., and P. N. Schumacher, 1999: *Mon. Wea. Rev.*, **127**, 2709-2732.